

**Magnetic Signature of an Above Ground Near One-Dimensional
Ferromagnetic Body Oriented Perpendicular to the Surface of The
Earth**

A Senior Thesis

Submitted as Partial Fulfillment of the Requirements

For the degree Bachelor of Science in

Geological Sciences at

The Ohio State University

By

Jason E. Kabbes

The Ohio State University, Summer Quarter, 2006

A handwritten signature in black ink, appearing to read "M. Barton", is written over a horizontal line.

Dr. Michael Barton

Acknowledgements

I would like to thank the following people for their efforts in helping me through this endeavor:

Dr. Michael Barton who advised me through this, as well as many other aspects of my education

Dr. Jeff Daniels who presented me with this topic

Dr. Hal Noltimier who bestowed his knowledge of field surveying unto me and granted me the use of his magnetometer

Timothy Schmeckle for his invaluable field assistance

Mohammad Azgarzadeh for his help generating maps.

Abstract

A study has been conducted to examine the effect a near one-dimensional rod-like ferromagnetic object oriented accurately in the z-direction (perpendicular to the surface of the Earth) had on the total magnetic field of its surrounding area. The total induced field was measured using a proton recession magnetometer. The data collected was used to generate maps showing the magnetic signature of the object. The amount of iron in the object was quantified, as to provide some guideline to the level of interference one can expect when taking magnetic data near above ground magnetically susceptible objects.

Introduction

The following study was conducted to examine the effect of an above ground rod-like object oriented in the z-direction (such as a flagpole) had on its surrounding area. The objectives of this study were twofold: (1.) To examine the difference(s), if any, an above ground object's magnetic signature has compared to a below ground object (2.) To gain a general idea as to how much interference one can expect when magnetically surveying an area with magnetically susceptible objects in plain sight. Naturally, the latter will be useful to environmental studies or surveys, but will provide little to no insight when mapping structures in the sub-surface such as dykes or sills.

Past studies have been conducted on below ground objects, both at shallow and great depths; however, few studies have been done on objects above the surface where the magnetometer actually sweeps below the anomalous object.

Equipment

Once the objective of the experiment was set, the first real task to overcome was finding a suitable object to create the anomalous/induced field. The object had to fit two criteria in order to be useful. First, the object had to be light and portable because the entire apparatus needed to be able to be quickly assembled and disassembled. This factor was very important in limiting error in the data due to diurnal drift (as The Sun passes over the surveyed area, it is constantly pushing and pulling on the magnetic field of The Earth.) If error was to be limited, all data needed to be collected in a timely manor, reducing the amount of drift and associated data correction (discussed later). Second, the object had to have large enough magnetic susceptibility to create a significant, measurable change in the total field. The reasoning behind the second criteria was the induced field had to be large enough to view and compare similarities/differences in the directional components of the field (compare east side of field to west side, etc.) It was obvious that a ferromagnetic body was most suitable, in that ferromagnetic bodies have a much larger susceptibility than diamagnetic or paramagnetic ones (Reynolds, 1997). After looking into several types of ferromagnetic materials such as nickel, cobalt, and iron, it was decided that one to several bars of iron-rebar was most suitable.

The iron content of the rebar needed to be tested to both ensure ferromagnetization and to loosely quantify the amount of iron that was to be examined. Two samples of rebar were sawed from separate ends of a bar to ensure the object was uniformly magnetized throughout. The samples were then tested by Energy Dispersive Spectroscopy (EDS). EDS spectral analysis is achieved by bombarding a sample with an

electron beam, shifting the electrons in the sample to a higher energy excited state. When they return to their original lower energy position/orbital, the energy difference generated from the excitation is emitted in the form of an x-ray. Each x-ray emitted has a characteristic wavelength that is intrinsic to the element and orbital from which it was derived (Goldstein, 2003).

Both samples contained approximately 97.5 % iron, 1.5 % manganese, and 1% silicon by weight. The manganese impurity is due to the atomic similarities between manganese and iron, where manganese can easily occupy iron sites in the short range atomic order of the alloy. The manganese impurity is very difficult to remove from samples containing iron, basically making it an inherent feature in iron samples (Oh, 1989). While it is possible that a small amount of silicon was present in the sample, it is probable that the silicon peak observed in the spectral curve was due to an x-ray(s) emitted from an iron atom hitting the quartz (SiO₂) sample window on the way into the detector (see Figure 1). This would have excited the silicon, generating silicon x-rays to be read by the detector, thus giving a faulty silicon peak. This process proved that both samples contained 97.5-98.5 wt. % iron, deeming the object both truly and uniformly ferromagnetic.

Once it was decided that the rebar would serve as a worthy material, the object had to be constructed. In that the magnetic profile to be taken had to sweep below the object, the rebar needed to be suspended somehow. To achieve this, four 3.5 kg bars of rebar measuring 3.2 meters length and 5cm diameter were duct taped together and placed into a PVC pipe also measuring 3.2 meters in length with 1 meter of rebar sticking out the end of the pipe. The diameter of the PVC was basically the diameter of the four bars,

ensuring the bars would be straight as long as the pipe was straight. The rebar was then taped to the PVC. When standing upright, the entire object stood 4.2 meters tall, with the bottom meter consisting of PVC only. This made it possible for the magnetometer, which stood at 0.8 meters, to truly sweep *below* the object.

The other piece of equipment was the Proton Precession Magnetometer, a type of magnetometer that is very common and easy to use. It consists of three basic parts: the sensor, the pole on which the sensor rests, and the analyzer. The sensor consists of a proton rich liquid (water) surrounded by a conductive coil, usually made of copper. Each proton in the liquid has its own magnetic moment and an angular momentum (Ripka, 2001). When the protons are subjected to an ambient field, such as The Earth's magnetic field, they align themselves parallel or anti-parallel with it. When an electric current is applied to the coil, it generates an applied magnetic field (as all charged coils do) that is perpendicular to the Earth's magnetic field. The protons in the liquid then align themselves with this new applied field. When the current is switched off, the protons precess around the pre-existing field at a specific frequency. As they precess, they induce a voltage back into the coil which is proportional to the strength of the applied field (Reynolds, 1997). The analyzer then converts the voltage into magnetic field strength and the total field is read.

The Experiment

The procedure of the experiment was quite simple. In that the object was portable, I was able to measure the field with and without the anomaly. I first measured the field without the object, to get a “normal” field for the area of interest. Once that was obtained, I erected the object and measured the field with it in place. The difference of the two fields was the magnetic effect of the object.

My surveyed field was at the Park of Roses in Worthington, Ohio. The experiment was conducted in the furthest possible space from the parking lot, as not to get any interference from cars, etc. The magnetic field of this area was rather constant, making it an ideal spot to conduct the experiment. Once it was decided the area would suffice, it then had to be gridded in one-meter increments. I chose a square grid that extended from the center point (the point which the object would sit) 20 meters in each cardinal direction, measuring each point and marking it with white spray paint. The total gridded area was 40 meters by 40 meters.

The next step was choosing a base station (approximately 40 meters to the east of the center of the grid) and recording its field. This was done to monitor the overall strength of the field with respect to the time data was being collected. This would later be used to adjust the data according to the diurnal effect of the sun as it crossed over my survey area, pushing and pulling the total field quite frequently. Base station readings had to be taken as often as possible to keep the data sound. This process will be discussed in more detail later.

I then read the total field of the survey area without the object in place, giving a “normal field” that I would later subtract from the induced field, giving the effect of the

object. I divided the area into four quadrants and took a base station reading between each quadrant. Once the data was adjusted, I found the magnetic field to be quite constant. Most points registered at 54,250 gammas, with a couple points on the eastern side reading 54,248 (see Figure 2). Now that the normal field was read, I could erect my object and record the induced field.

To accurately erect the PVC/rebar, a series of ropes were taped to the object, pulled taught, and staked down with plastic stakes. To ensure the accuracy of the object, a participant constantly held the bar (as to not let it shift with wind, etc) and checked it with a plastic level every 5 minutes. The instrument would not give a reading within 1.5 meters of the object, so I started each quadrant at the 2-meter point and moved out recording the time at each point. As earlier, base station readings were done between each quadrant. The total field was recorded (see Figure 3) and the fieldwork of the experiment was complete.

Data and Data Adjustment

As stated, the Earth's magnetic field changes over a daily period. This is caused by changes in the direction and strength of currents in the ionosphere (Reynolds, 1997). These changes are greatest near the geomagnetic equator and decrease toward the magnetic poles (Joyce, 1937). There exists an observable trend in this change of field strength. In the middle of the night, the field is ambient with little change. The amplitude of change decreases from dawn to midday, increases to its daily maximum in the late afternoon, then slowly settles to the night-time value (Reynolds, 1997). This process continues day by day, with some days having drastic changes in amplitude, while

others have relatively small ones. While the overall trend may seem smooth and continuous, small changes occur minute by minute and seem to oscillate around an hourly average. This can be rather problematic when surveying many points, further displaying the need for numerous base station readings.

Because of these changes, it is quite necessary to adjust all data to fit a single point in time. I chose the beginning of the experiment to be my fixed point in time, when the magnetic field of the base station was 54,245 gammas. Eventually, all data was adjusted as if it was taken at the point in time when the base station was at 54,245 (see Figure 4). One of the drawbacks of the magnetometer used is the amount of time it takes to get a group of readings. Therefore, the normal field varied a great deal throughout the course of the experiment and would have caused confusion among the data if it was not adjusted. To adjust all data to fit one fixed point in time, a series of simple calculations had to be done. I first calculated the change in gammas per minute along each series of data (quadrants) and adjusted it to the base station at the beginning of the quadrant. If the base station had dropped from 54,261 to 54,251 from 3:56 to 4:01, a change in 10 gammas over five minutes had occurred (see Figure 4). Therefore, I added 2 gammas per minute after time $t = 0$, making all data points seem as though they were read at the point in time when base station was 54,261. Once each quadrant was adjusted to fit the base station reading taken at the beginning of that quadrant, I either added or subtracted to fit all data to when base station was at 54,245. Now my data was sound and I could construct my figures.

The induced field showed a positive anomaly to the south of the object. The peak of the anomaly had to be inferred because I could not get a reading close to the object. At

two meters to the south, the field had increased to 54,704 gammas, approximately 450 gammas above the normal field. It decreased 250 gammas along the next meter, then 125 over the next, giving a reading of ~54,325 at the fourth meter to the south. The field then decreased gradually until it reached the norm at ~18 meters from the object (see figures 5 and 6).

A negative anomaly was read on the north side of the object, again with the peak unreadable. The field was only 3 gammas below the norm at two meters to the north, rose to about 125 above the norm at ~2.5 meters, then dropped to the norm at ~9 meters. The profile from south to north did, in fact, follow the convention of negative anomaly to the south and positive to the north. The east and west sides were basically symmetrical, giving a reading of 54,460 at two meters to either side. The field dropped dramatically to 54,283 at five meters, then decreased gradually, reaching the norm at ~9 meters.

Conclusions

After examining data and figures, it is apparent that the induced field of a magnetically susceptible anomalous object in the Northern Hemisphere will yield a positive anomaly to the south and a negative anomaly to the north, regardless of whether the reading is taken above or below the object, or whether the object is buried.

The peaks of the profile were very narrow, which makes sense because wavelength of a doublet peak is proportional to the distance between the magnetometer and the magnetic object. Had the object been raised higher, the peaks would be less intense and more stretched out.

The observed positive anomaly starting three meters to the north of the object is often seen in observed and corrected data (Reynolds, 1997).

The induced field was stretched further to the south (18m) than the north (9m). This concludes that any individual taking magnetic field readings can expect greater interference on the south side of objects than the north side. If further study is to be done, numerous amounts of iron should be used and some plot should be generated to display amount of interference (in gamma or nano-tesla) as a function of iron content and distance to object. It would also be useful to study induced field strength as a function of orientation of the object, as I found the field to stretch and decrease in amplitude as the body was tilted.

Limitations

The proton magnetometer is very limited, in that it takes much time to get a series of readings. More contemporary models continuously take and store data, reducing diurnal effect.

Although effective, the data correction assumed a linear change in field strength between base station readings, when the change could exist exponentially.

Figure 6 contains four features in the outer most contour. These features could not be gotten rid of and are an effect of the software used to generate the map.

References

Reynolds, J.M. An Introduction to Applied and Environmental Geophysics. John Wiley and Sons Ltd., West Sussix, England, 1997. Chapter 3 p 123-158

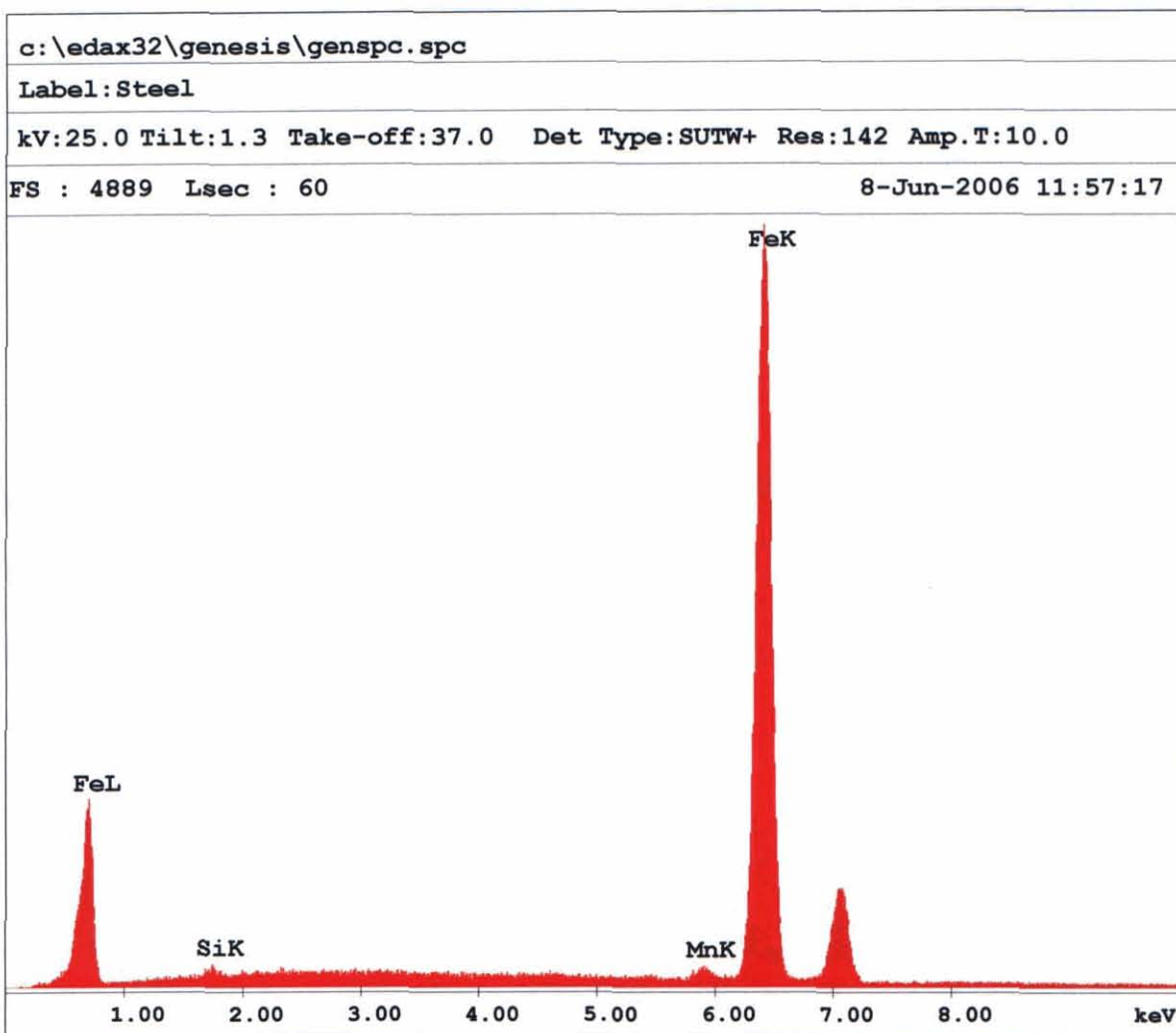
Goldstein, J., Newbury, D., Joy, D., Lyman, C., Echlin, P., Lifshin, E., Sawyer, L., Michael, J. Scanning Electron Microscopy and X-Ray Microanalysis. Kluwer Academic/Plenum Publishers, New York, New York, 2003. Chapter 7 p 297-350

Oh, J.M., Glenn, M.L. Structural Stability and Oxidation Resistance of Substitute Alloys with Various Chromium and Manganese levels. United States Department of the Interior, Bureau of Mines, Pittsburgh, PA, 1989

Ripka, P. Magnetic Sensors and magnetometers. Artech House, Boston, 2001. Chapter 7 p 271-289

Joyce, J.A. Manual on Geophysical Prospecting with Magnetometers. American Askania corporation under a cooperative agreement with the United States Bureau of Mining, 1937.

Spectral Analysis of Iron Sample



EDAX PhiRhoZ Quantification (Standardless)
 Element Normalized
 SEC Table : User c:\edax32\eds\genuser.sec

Element	Wt %	At %	K-Ratio	Z	A	F
SiK	0.84	1.65	0.0034	1.1384	0.3526	1.0020
MnK	1.43	1.44	0.0139	0.9805	0.9929	1.0000
FeK	97.74	96.91	0.9762	0.9990	0.9998	1.0000
Total	100.00	100.00				

Element	Net Inte.	Bkgd Inte.	Inte. Error	P/B
SiK	9.05	11.43	8.06	0.79
MnK	15.58	11.07	5.09	1.41
FeK	962.85	9.30	0.42	103.53

Figure 1

Field strength
(gamma)
w/out
anomaly

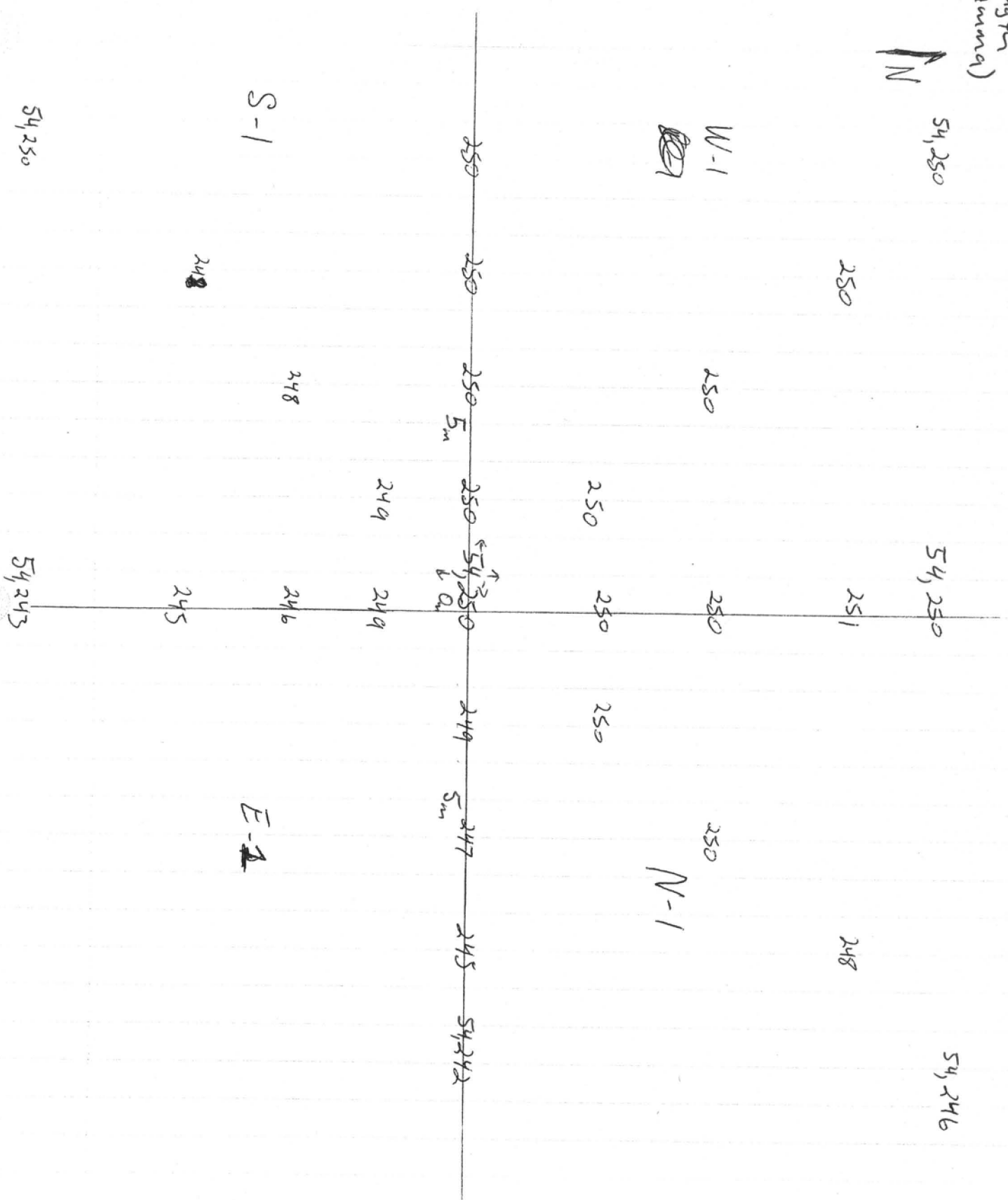


Figure 2

Field strength
(gamma)

W/
Anomaly

W-2

IN

S-2

54,250

54,251

54,270

54,505

54,247

54,343

54,268

54,248

54,246

N-2

250 250 250 254 268 272 283 314 368 460 450 370 313 281 270 265 247 245 244 242
(10) (5) (5) (10)

54,406

54,704

54,402

54,275

5) 298

54,274

E-2

54,256

10) 264

54,254

54,250

260

54,250

BS

3:11 54,245
3:16 54,244
3:21 54,251
3:24 54,251
3:28 54,251
3:36 ~~54,252~~
3:56 54,259
4:10 54,262
4:24 54,257
4:34 54,255
4:50 54,265

251 (15)

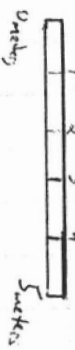
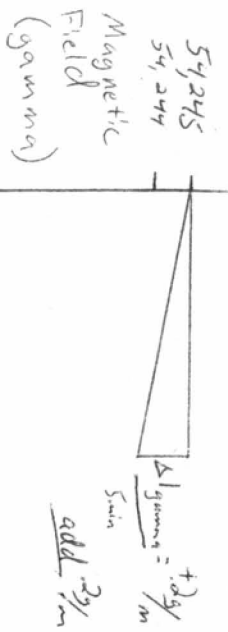


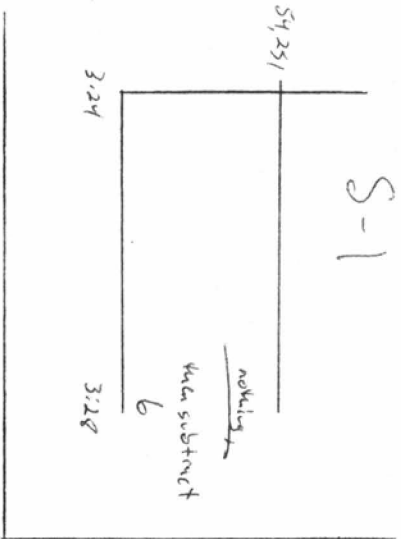
Figure 3

W-1

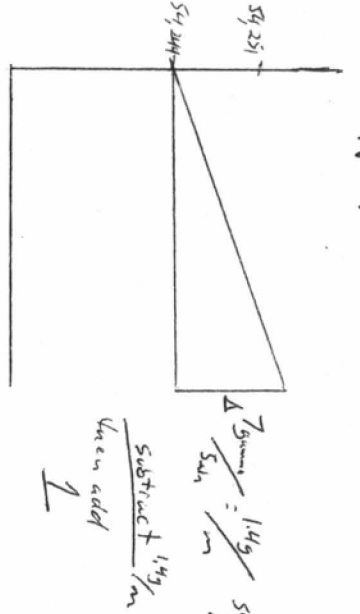


Still time (minutes)

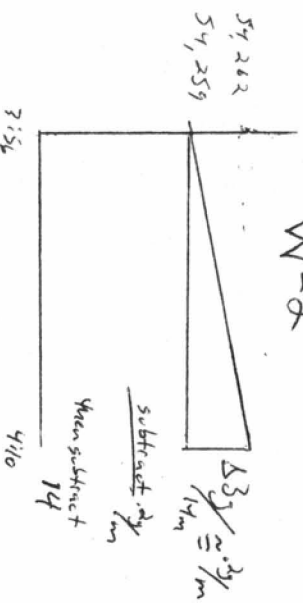
S-1



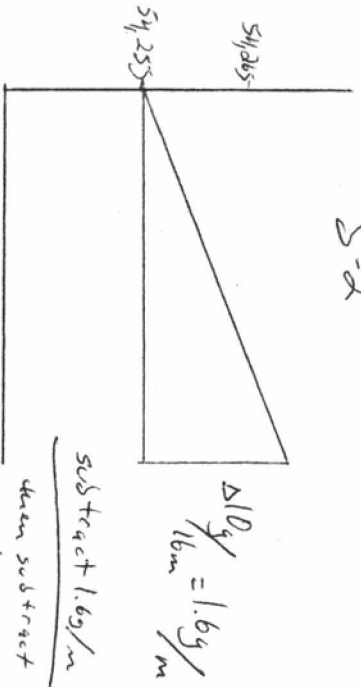
N-1



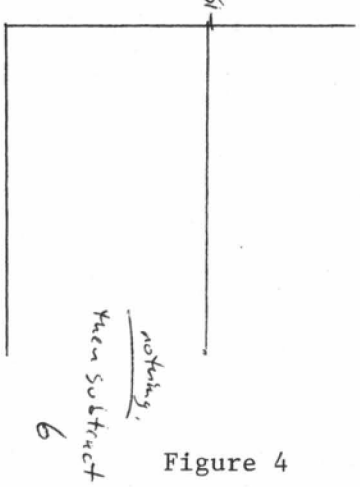
W-2



S-2



E-1



N-2

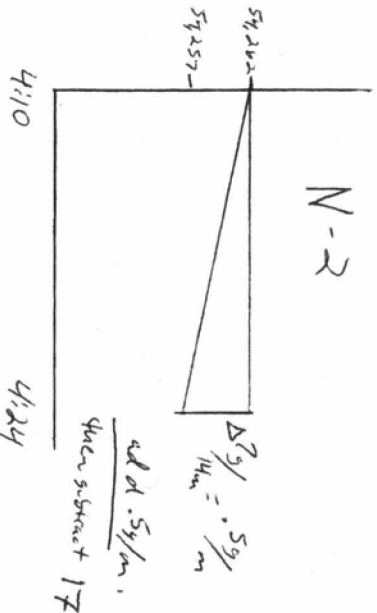


Figure 4

Data Correction
For DIURNAL SHIFT

X-section from S to N

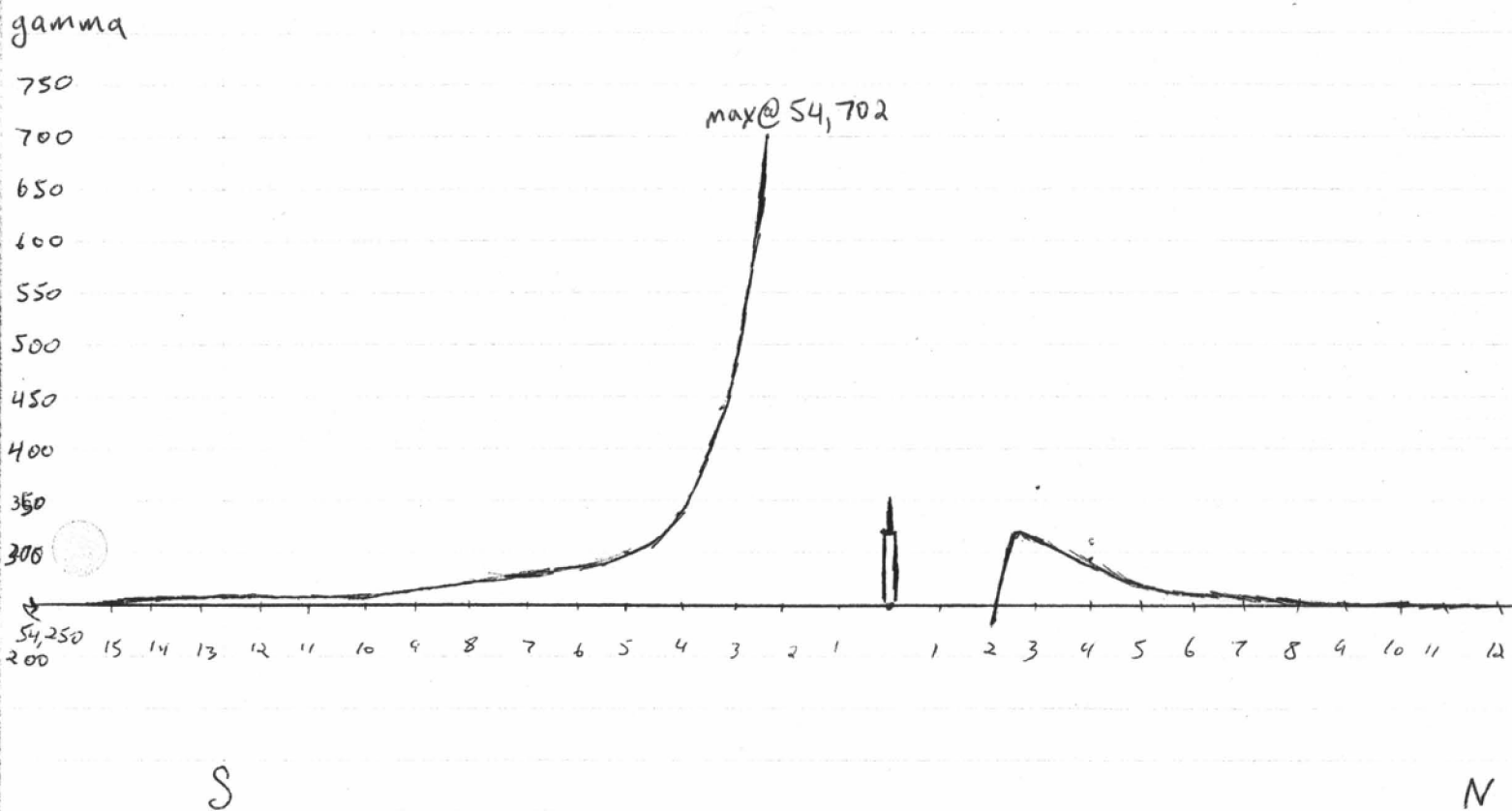


Figure 5

2-Dimensional representation of magnetic data using surfer

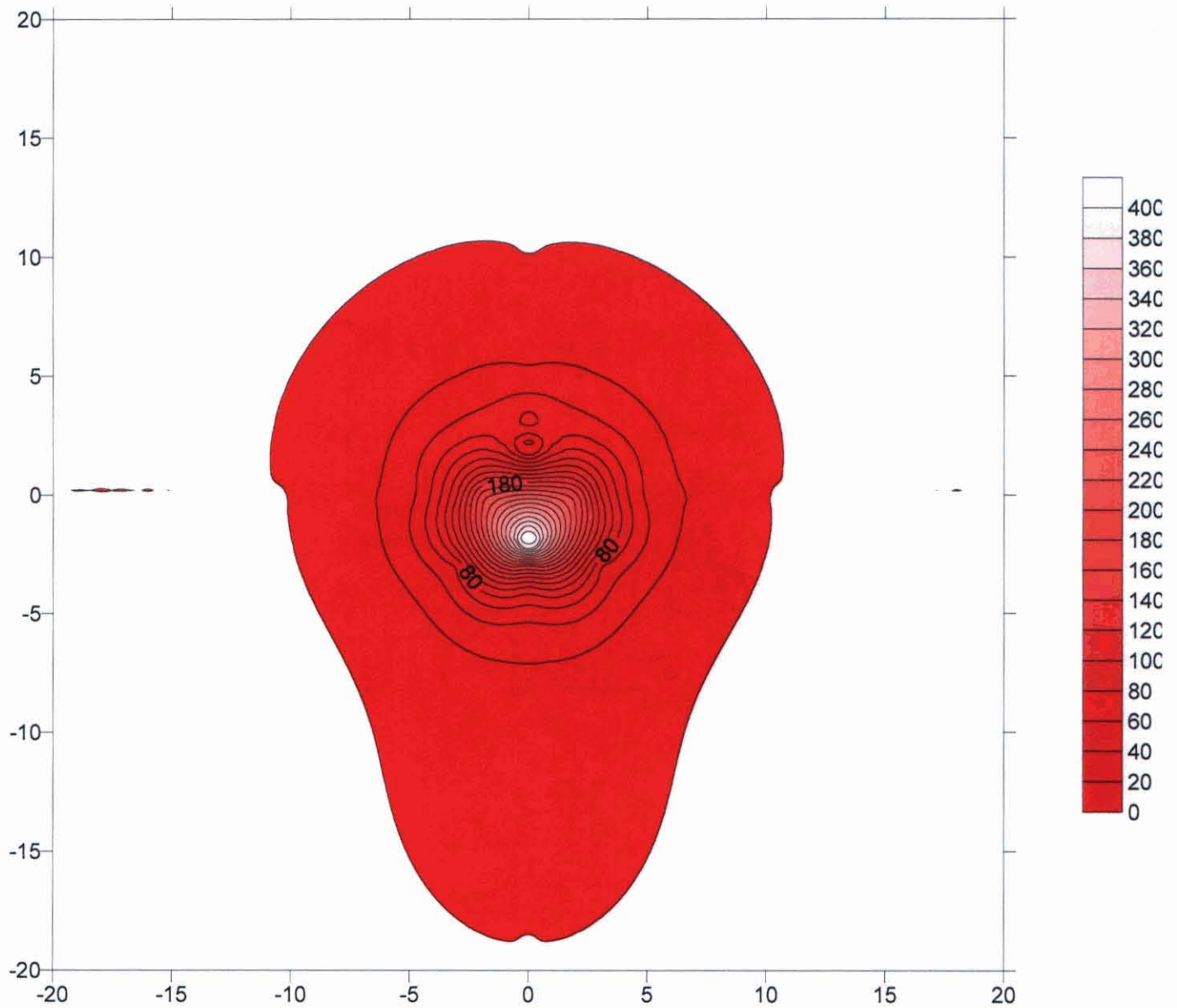


Figure 6

3 Dimensional Visualization of Magnetic Data using MATLAB 6.5

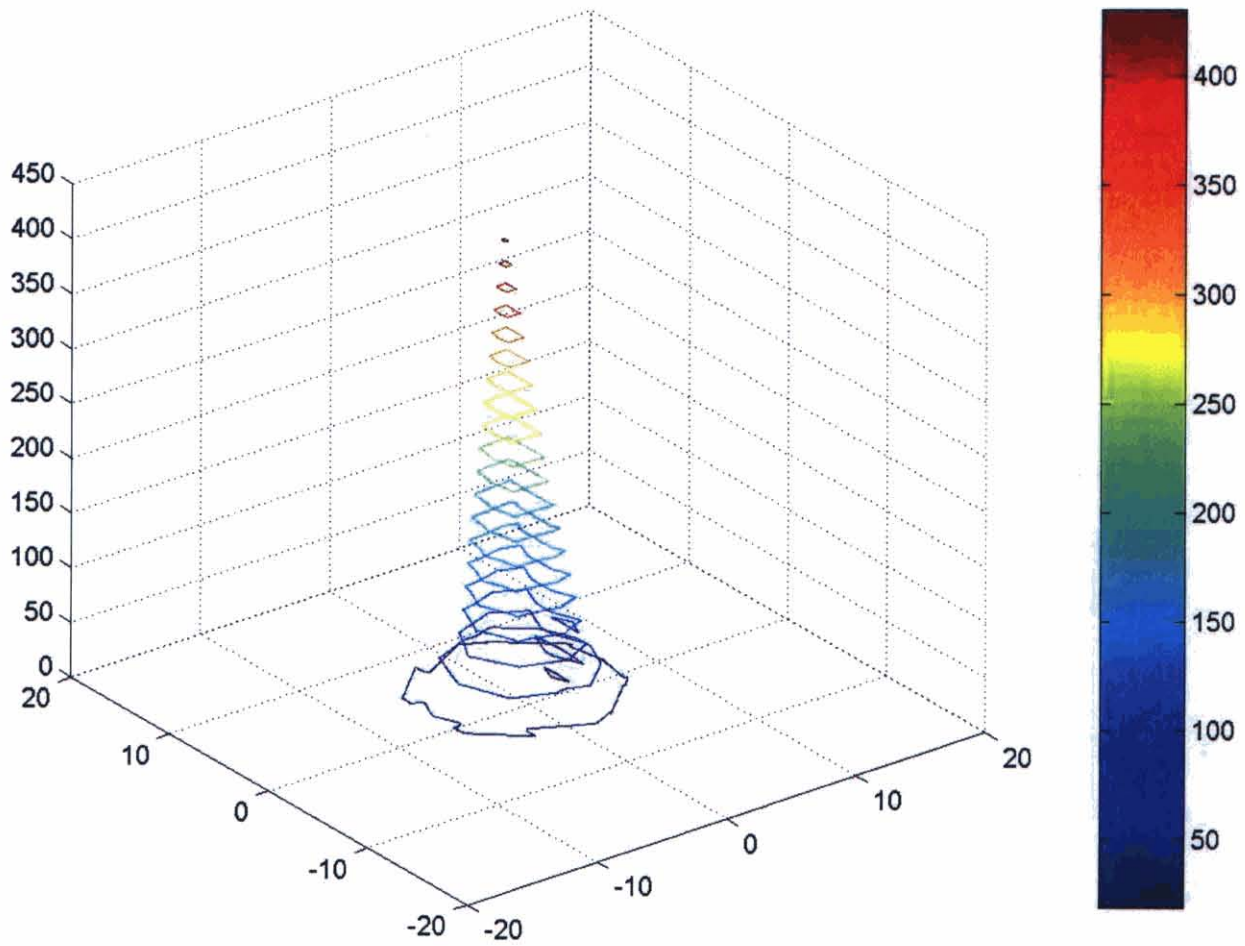


Figure 7

X	Y	Z
2	0	212
0	2	-3
0	6	17
-20	0	0
-19	0	0
-18	0	0
-17	0	0
-16	0	0
-15	0	0
-14	0	0
-13	0	0
-12	0	0
-11	0	0
-10	0	0
-9	0	2
-8	0	4
-7	0	18
-6	0	22
-5	0	33
-4	0	64
-3	0	118
-2	0	210
2	0	212
3	0	120
4	0	66
5	0	35
6	0	23
7	0	19
8	0	5
9	0	2
10	0	0
11	0	0
12	0	0
13	0	0
14	0	0
15	0	0
16	0	0
17	0	0
18	0	0
19	0	0
20	0	0
0	2	-3
0	3	73
0	4	47
0	5	23
0	6	17
0	7	9
0	8	6
0	9	1
0	10	0
0	11	0

0	12	0
0	13	0
0	14	0
0	15	0
0	16	0
0	17	0
0	18	0
0	19	0
0	20	0
0	-2	452
0	-3	191
0	-4	87
0	-5	48
0	-6	30
0	-7	21
0	-8	15
0	-9	14
0	-10	14
0	-11	12
0	-12	10
0	-13	8
0	-14	6
0	-15	5
0	-16	3
0	-17	2
0	-18	0
0	-19	0
0	-20	0
-3	-3	63
-4	-5	23
-3	2.5	50
-3	5	20
-6	1.65	20
3	-3	63
4	-5	23
3	2.5	50
3	5	20
6	1.65	20

0	12	0
0	13	0
0	14	0
0	15	0
0	16	0
0	17	0
0	18	0
0	19	0
0	20	0
0	-2	452
0	-3	191
0	-4	87
0	-5	48
0	-6	30
0	-7	21
0	-8	15
0	-9	14
0	-10	14
0	-11	12
0	-12	10
0	-13	8
0	-14	6
0	-15	5
0	-16	3
0	-17	2
0	-18	0
0	-19	0
0	-20	0

X	Y	Z
2	0	212
0	2	-3
0	6	17
-20	0	0
-19	0	0
-18	0	0
-17	0	0
-16	0	0
-15	0	0
-14	0	0
-13	0	0
-12	0	0
-11	0	0
-10	0	0
-9	0	2
-8	0	4
-7	0	18
-6	0	22
-5	0	33
-4	0	64
-3	0	118
-2	0	210
2	0	212
3	0	120
4	0	66
5	0	35
6	0	23
7	0	19
8	0	5
9	0	2
10	0	0
11	0	0
12	0	0
13	0	0
14	0	0
15	0	0
16	0	0
17	0	0
18	0	0
19	0	0
20	0	0
0	2	-3
0	3	73
0	4	47
0	5	23
0	6	17
0	7	9
0	8	6
0	9	1
0	10	0
0	11	0

0
0
0
0
0
0
0
0
0
0
0
0
1
6
9
17
23
47
73
-3

212 120 65 35 24 20 5

452
191
87
48
30
21
15
14
14
12
10
8
6
5
3
2
0
0
0

0

0

2

0

0

0

0

0

0

0

0

0

0